Journal of Chromatography A, 1603 (2019) 8–14

Contents lists available at ScienceDirect

Journal of Chromatography A

journal homepage: www.elsevier.com/locate/chroma

Low cost 235 nm ultra-violet light-emitting diode-based absorbance detector for application in a portable ion chromatography system for nitrite and nitrate monitoring

Eoin Murray[a,b], Patrick Roche[a], Kevin Harrington[a], Margaret McCaul[b], Breda Moore[a], Aoife Morrin[b], Dermot Diamond[b], Brett Paull[c,d,*]

[a] Research & Development, T.E. Laboratories Ltd. (TelLab), Tullow, Carlow, Ireland
[b] Insight Centre for Data Analytics, National Centre for Sensor Research, School of Chemical Sciences, Dublin City University, Dublin 9, Ireland
[c] Australian Centre for Research on Separation Science (ACROSS), School of Physical Sciences, University of Tasmania, Sandy Bay, Hobart 7001, Australia
[d] ARC Training Centre for Portable Analytical Separation Technologies (ASTech), School of Physical Sciences, University of Tasmania, Sandy Bay, Hobart 7001, Australia

ARTICLE INFO

Article history:
Received 3 March 2019
Received in revised form 7 May 2019
Accepted 19 May 2019
Available online 21 May 2019

Keywords:
Light-emitting diode
Deep UV
Ion chromatography
Nutrients
Water analysis
Portable

ABSTRACT

A low cost, UV absorbance detector incorporating a 235 nm light emitting diode (LED) for portable ion chromatography has been designed and fabricated to achieve rapid, selective detection of nitrite and nitrate in natural waters. The optical cell was fabricated through micromilling and solvent vapour bonding of two layers of poly (methyl methacrylate) (PMMA). The cell was fitted within a 3D printed housing and the LED and photodiode were aligned using 3D printed holders. Isocratic separation and selective detection of nitrite and nitrate was achieved in under 2.5 min using the 235 nm LED based detector and custom electronics. The design of the new detector assembly allowed for effective and sustained operation of the deep UV LED source at a low current (<10 mA), maintaining consistent and low LED temperatures during operation, eliminating the need for a heat sink. The detector cell was produced at a fraction of the cost of commercial optical cells and demonstrated very low stray light (0.01%). For retention time and peak area repeatability, RSD values ranged from 0.75 to 1.10 % and 3.06–4.19 %, respectively. Broad dynamic linear ranges were obtained for nitrite and nitrate, with limits of detection at ppb levels. The analytical performance of the IC set up with optical cell was compared to that of an ISO-accredited IC through the analysis of five various water samples. Relative errors not exceeding 6.86% were obtained for all samples. The detector was also coupled to a low pressure, low cost syringe pump to assess the potential for use within a portable analytical system. RSD values for retention time and peak area using this simple configuration were <1.15% and <3.57% respectively, highlighting repeatability values comparable to those in which a commercial HPLC pump was used.

1. Introduction

Nitrogen in the form of nitrite (NO_2^-) and nitrate (NO_3^-) is naturally found in environmental waters. These anions play an integral role in facilitating the growth of algae and flora essential for aquatic ecosystems. Despite their intrinsic nature within environmental waters, excessive levels of nitrate and nitrite, as a consequence of point and nonpoint pollution sources derived from anthropogenic activities, present a notable risk to both environmental and human health [1]. Both nitrite and nitrate contribute to eutrophication which results in the over-production of algae and aquatic plants. Algal blooms readily produce toxins and bacteria which are harmful to human health. These blooms can also severely reduce oxygen levels in water which has a detrimental impact on aquatic life. In addition to environmental impacts, nutrient pollution also has a significant economic impact. In the U.S. alone, nutrient pollution is estimated to cost $2.2 billion dollars per year [2] and this economic impact can be reflected across the globe [3].

A broad range of standard analytical techniques exist for the analysis of nitrite and nitrate in water samples [4,5], the most common of which being colorimetry and suppressed ion chromatography (IC) [6–8]. Under global legislation, such as the Water

* Corresponding author at: Australian Centre for Research on Separation Science (ACROSS), School of Natural Sciences, University of Tasmania, Sandy Bay, Hobart, 7001, Australia.
E-mail address: Brett.Paull@utas.edu.au (B. Paull).

https://doi.org/10.1016/j.chroma.2019.05.036
0021-9673/

Framework Directive (WFD) within Europe and the U.S. Clean Water Act, the concentrations of nitrate and nitrite within environmental waters must be monitored. In order to achieve truly effective water quality management, deployable *in-situ* sensor systems capable of achieving high frequency and spatial data are required. With the advent of rapid prototyping technologies, such as 3D printing and micro-milling, a number of *in-situ* nitrite and nitrate analysers have been reported [9,10]. Yet these technologies remain poorly implemented and have not seen widespread adoption for aquatic nutrient monitoring [11]. Leading *in-situ* analysers for nitrate and nitrite employ colorimetric chemistries coupled with visible light emitting diode (LED) based optical detection [9,12]. These analysers require multiple reagents which can be affected by temperature, and for nitrate detection, require a reducing agent such as cadmium or vanadium chloride adding further complexity. A number of *in-situ* analysers which perform direct UV absorbance detection of nitrate are also commercially available, however these systems exist at a significant price point and have high power consumption requirements due to the use of a UV deuterium lamp [13,14]. Current technological limitations and prohibitive costs have hampered robust *in-situ* systems from becoming routinely used and adopted on a large scale. [11].

Over the past decade, LEDs have seen increasing use within optical detectors across a broad range of applications within analytical chemistry [15]. Their low-cost (relative to traditional lamps), low power consumption, small size, robustness and narrow emission bandwidth, make them ideal for use within portable, miniature and deployable analytical systems. As mentioned above, until now, most nutrient analysis systems and approaches, which employ LEDbased detection, do so in conjunction with colorimetric chemistries in the visible or near UV spectrum, typically focused on nitrate, nitrite and phosphate detection [16,17]. However, LEDs emitting in the deep-UV range (<280 nm) have recently become more readily available [18] and have now been applied for absorbance detection in combination with a range of analytical techniques, *e.g.* HPLC, ion chromatography (IC) and capillary zone electrophoresis (CZE), for the detection of organic and inorganic analytes [19–22]. Given that nitrite and nitrate have maximum absorption wavelength values (λ_{max}) of 209 and 200 nm respectively [23], a deep-UVC LED of <240 nm is required to enable direct absorbance-based detection of these species. Recently, Li et al. 2016 [24] demonstrated for the first time the use of a 235 nm LED for chemical analysis, performing direct absorbance detection of nitrate and nitrite using standard capillary IC coupled with a modified on-capillary detector, comprising of a commercial optical interface. Within this detector set up, the LED required relatively high currents to generate sufficient light intensity for operation on a capillary scale. This high current saw increased LED temperatures, and as LED performance, lifetime and emission wavelength are negatively affected with increasing temperature, a heat sink for heat dissipation was required [25]. Similarly, Silveira Petruci et al. [26] demonstrated the use of a 235 nm LED for direct detection of organic analytes with standard commercial HPLC and again a heat sink was required for analysis. For portable low-cost instruments this additional requirement, albeit passive or active, adds unwanted complexity to the detector cell, which potentially could be avoided.

In this work, we describe an alternative deep-UV low-cost detector design, and demonstrate its simplicity and performance when applied as the optical detector within a portable IC system for nitrite and nitrate monitoring. The detector itself was fabricated using rapid prototyping techniques, including micromilling and 3D printing, and incorporates a 235 nm deep-UV LED with a UV photodiode for the direct detection of nitrite and nitrate. Rapid separation of the anions is achieved using a low backpressure (<12 bar) IC method. The new design of the optical cell eliminates the need for heat sinks or heat dissipation and this is demonstrated through a thermal study of the LED within the optical detector during one hour of continuous operation. Without the need for a heat sink, complexity and manufacturing time associated with the optical detector is reduced. Custom electronics were used with the detector facilitating portability and again enabling a reduction in system cost. The stray light and effective path length of the fabricated optical cell was determined, along with the analytical performance and chromatographic repeatability. Environmental samples and blind standards were also analysed using the prototype instrument to establish the analytical accuracy when using direct UV absorbance. Finally, low cost eluent syringe pumps were fabricated and tested with the developed method and detector to demonstrate the potential for implementation within a portable format.

2. Experimental

2.1. Chemicals and reagents

All chemicals employed within this work were of analytical or higher grade. All solutions and dilutions were prepared using high-purity deionised water (Milli-Q). Potassium hydroxide used as the eluent was purchased from Sigma-Aldrich (St. Louis, MO). Nitrite and nitrate stock solutions were prepared using $NaNO_2$ and KNO_3 salts respectively (Sigma-Aldrich, St. Louis, MO). For the interference study, fluoride, chloride, iodide, iodate, bromide, phosphate, sulphate and carbonate stock solutions were prepared using NaF, NaCl, KI, KIO_3, KBr, KH_2PO_4, K_2SO_4 and K_2CO_3 salts respectively (Sigma-Aldrich Co., St. Louis, MO). Orange G used within the optical study of the detector cell was obtained from Fluka (Buchs, Switzerland). Working standards were prepared through dilution of stock solutions. The environmental samples, along with the Environmental Protection Agency (EPA) inter-calibration standard, were provided by the Environmental Department within TelLab (Carlow, Ireland).

2.2. Instrumentation

For initial method development a Thermo Fisher Scientific Ultimate 3000 HPLC pump was used to deliver 100 mM KOH eluent at a rate of 0.8 mL min^{-1}. The pump was coupled to a manual 6 port 2-position high pressure injection valve provided by VICI AG (Schenkon, Switzerland). Rapid separation was achieved using a 4 × 50 mm Dionex AG15 guard column from Thermo Fisher Scientific (Sunnyvale, CA). The 235 nm deep UV-LED used for absorbance detection was provided by Crystal IS (Green Island, NY, USA). A UVC photodiode (TOCON_C1) with integrated amplifier employed for photodetection was purchased from Sglux GmbH (Berlin, Germany). For the analytical comparison study, nitrate and nitrite concentrations in environmental and blind samples were determined using an accredited Dionex DX-120 Ion Chromatograph (Dionex, Sunnyvale, USA), equipped with autosampler and a Dionex AERS 500 anion self-regenerating suppressor for suppressed conductivity detection. The low-pressure eluent syringe pumps which were used in the final application and the detector itself were designed using Fusion 360 computer aided design software (Autodesk Inc., California, USA). Syringe pump drive plates and back plates were made using Onyx filament sourced from Markforged, Inc. (Massachusetts, USA) and were printed using a Markforged Mark Two printer. The syringes used were 1 mL gas tight luer lock glass syringes sourced from Sigma-Aldrich (Wicklow, Ireland). Flushing of syringes was achieved through the use of 12 V brushed geared DC motors (Pololu, Las Vegas, USA) connected to an Aim-TTi EL303R power supply (RS Radionics, Dublin, Ireland). Rod collars and motor couplings were also provided by RS Radionics.

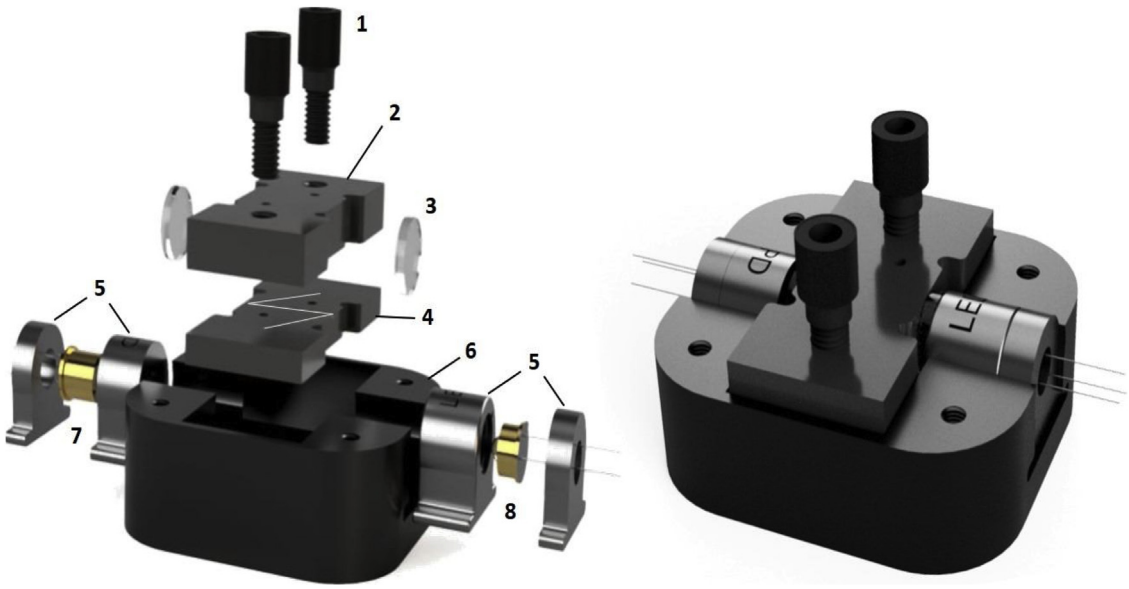

Fig. 1. Design of the low-cost UV absorbance detector (left) and illustration of assembled detector (right). Legend: (1) flangeless nut fittings; (2) top PMMA layer with milled, threaded holes for cell inlet and outlet; (3) fused silica glass UV-transparent windows (12.5 × 2 mm); (4) bottom PMMA layer with milled z-shape fluidic channel; (5) 3D printed holders for LED and photodiode; (6) 3D printed optical cell holder; (7) photodiode; (8) 235 nm LED.

Operation of the LED and photodiode along with data acquisition was achieved using in-house customised electronics, comprised of electronic components sourced from Mouser Electronics (Texas, USA). Functionality was enabled through the use of an 8-bit Arduino microcontroller (ATMEGA2560). The LED was powered using a constant current driver (AL8805) with a PWM (pulse width modulation) signal used to control the intensity of light emitted. The resultant analogue signal from the UVC photodiode was sent to a 16-bit analogue to digital converter (ADS1115). Raw bit values produced by the analogue to digital converter were filtered with a 15-point running average and data was then sampled at a frequency of 20 H Chromatographic data were transmitted *via* serial port to a PC for real-time visualisation of the data using Arduino serial plotter. Data generated for each sample were arranged into a comma separated value (CSV) format and were stored on a microSD card in a CSV file for post processing. Absorbance (AU) values were obtained using the equation of $AU = -\text{Log}_{10}(V_S)/(V_B)$, where V_S was the voltage signal generated by the photodiode following sample injection and V_B was the baseline voltage signal. Origin data analysis software was used for processing of chromatograms and peak area integration (OriginLab Corportaion, MA, USA).

2.3. UV optical detector

The custom designed optical detector (Fig. 1), based on a z-shape format, was fabricated using two layers of poly (methyl methacrylate) (PMMA) and was 50 × 25 x 12 mm in size. On the bottom PMMA layer a microfluidic z-shaped channel with a diameter of 500 μm and optical path of 2.15 cm was micro-milled. The internal volume of the z-cell channel was 11 μL. On the top PMMA layer two threaded openings were milled. One opening was used as an inlet and the second opening as the cell outlet. Micromilling of the PMMA was carried out by EFJ Engineering (Dublin, Ireland). The two PMMA layers were bonded through solvent vapour bonding, as described by Ogilvie et al. [27]. Following solvent bonding of the two PMMA layers, UV-transparent fused silica glass windows (Edmund Optics Inc., Barrington, NJ) were positioned and bonded at each side of the detector optical channel using epoxy putty obtained from J-B Weld (Sulphur Springs, TX). The detection cell was assembled within a 3D printed housing. The LED and photodiode were positioned and aligned at each window of the cell using custom 3D printed holders adapted from Donohoe et al. [28]. All 3D printing of components was carried out using a Markforged Mark Two printer. The total component cost for the UV optical detector, including the LED, photodiode and electronics for data acquisition and operation was < $430.

2.4. Stray light and effective path length determination

The procedure employed within this study was similar to that described by Li et al. 2016 [24]. The dye Orange G was used to demonstrate the detector linearity as an absorbance to concentration relationship. A sensitivity versus absorbance plot was generated with sensitivity being determined by dividing absorbance by concentration [29,24]. An Orange G stock solution was prepared and working standards were then made through serial dilution of the stock using DI water. Orange G standards, of concentrations ranging from 0.5 to 1000 μM, were used. Measurements were performed by flushing 5 mL of standard solution through the cell, the flow was then stopped and the absorbance was measured using the 235 nm LED under static flow conditions. Measurement of each standard solution was carried out in triplicate and in order of increasing concentration. Between each measurement of Orange G solution, the cell was flushed with 5 mL of DI water to prevent sample carry over. Percentage of stray light and the effective path length of the detector cell were calculated using the sensitivity versus absorbance plot as specified by Macka et al. [29].

3. Results and discussions

3.1. Thermal study of LED and detector

It has been established that thermal management of deep-UV LEDs is an important consideration when employed for analytical operations. High currents are typically applied during analysis using these LEDs and electrical power not converted into light is converted into heat. With increasing LED temperature, luminous efficiency decreases, emission wavelengths shift and LED lifetime is reduced [15]. In recent works in which the 235 nm LED was used

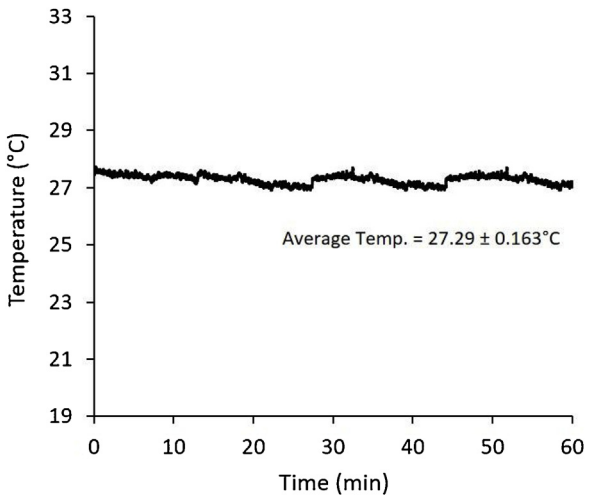

Fig. 2. Temperature measurement of 235 nm UV-LED within optical cell over 1 h of continuous operation, recorded using thermal camera. Temperature reading represents the temperature of the hottest point of the LED during operation.

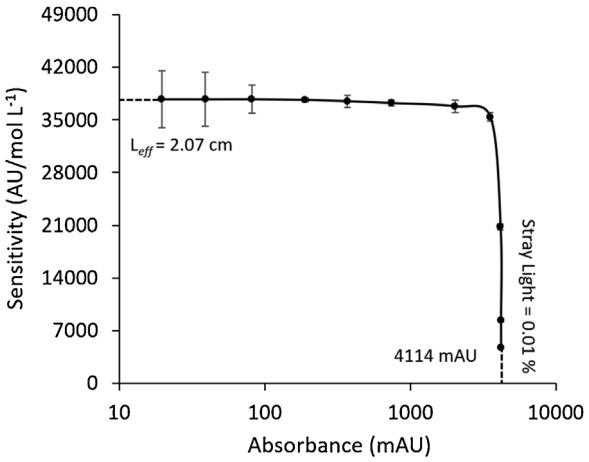

Fig. 3. Linearity of 235 nm LED-based detector illustrated as sensitivity versus absorbance plot (error bars are standard deviations for n = 3 replicates). A stray light value of 0.01% was estimated for the detector and an effective pathlength of 2.07 cm was calculated.

for optical detection with chromatography, the use of a heat sink for heat dissipation was required to achieve optimal analytical performance, as relatively high running currents of 100 mA [24] and 66 mA [26] were used to operate the LED.

Due to the 500 μm channel dimensions within the current cell and alignment of the LED and photodiode, which was achieved by the 3D printed holders and housing, it was found that effective operation and sensitivity could be achieved when driving the LED within the detector at a constant current of just 9 mA. Under these conditions, the background noise, determined by monitoring baseline signal for 60 s and recording maximum fluctuations, was just 0.25 mAU. This was comparable to the 0.30 mAU noise reported by Petruci et al. [26]. By operating the LED at this low current, the issue of LED overheating was eliminated and in turn an LED heat sink was not required. Temperature measurements of the 235 nm LED within the detector over one hour of continuous operation are shown in Fig. 2. The temperature reading was recorded from the point of the LED at which the highest temperature was observed. Thermal imagery of the LED and cell is shown in Fig. A1 of the electronic supplementary information (ESI). The average temperature of the hottest point of the LED during continuous operation was 27.29 ± 0.16 °C.

3.2. Detector stray light and effective optical path length

The stray light and effective path length associated with the fabricated UV optical cell was determined through the use of the azo dye Orange G. The effective pathlength and approximation of stray light were determined using the same approach set out by Li et al. [24] and others [30], in which the theoretical model based on Beer's law as reported by Macka et al. [29] is used. The effective pathlength (L_{eff}) and stray light were calculated using the plot of detection sensitivity (AU/mol L^{-1}) versus absorbance (Fig. 3). Extrapolation to the y-axis yielded a sensitivity value of 38,000 AU/mol L^{-1}. Using this estimated value along with the molar absorptivity value of Orange G (18,300 L mol^{-1} cm^{-1}), an effective pathlength of 2.07 cm was observed. This effective pathlength corresponded to 96.28% of the actual optical channel length of the detector (2.15 cm). The upper limit of detector linearity, herein set at the absorbance value corresponding to a 5% drop in sensitivity, was 3.162 AU. This observed upper linearity limit is similar to commercially available high sensitivity detection cells (detector linearity up to 2 AU), while at a fraction of the cost [31]. Following extrapolation to the x-axis, where sensitivity = 0, an absorbance of 4.114 AU was observed which corresponds to a negligible stray light level of <0.01%. This very low stray light level is most likely associated with the large optical path length and the non-transparency of the PMMA to UV light. The essentially zero stray light observed is very encouraging, when taken in comparison to other detection cells employing deep UV LEDs, such as the LED-based detector reported by Sharma et al. in which a stray light of 3.6% was reported [32]. Similarly, the lowest stray light reported by Li et al. for a high sensitivity UV LED-based detector incorporating commercial z-cells was 3% [21].

3.3. Chromatographic repeatability

The measurement repeatability associated with the LED-based optical detector combined with the IC set up was established through the analysis of an anion standard solution containing 0.5 mg L^{-1} NO_2^- and 2.5 mg L^{-1} NO_3^-. The anion standard was injected 30 consecutive times. The retention time and peak area repeatability for both analytes are graphically presented in Fig. 4. Relative standard deviations (RSD) of retention times and peak areas for the 30 runs ranged from 0.75 to 1.10 % and 3.06–4.19 %, respectively. Chromatographic repeatability is also illustrated in Fig. B1 of the ESI, as a selection of chromatograms from the 30 injections are overlaid. Despite the rapid separation, simple configuration and low-cost detection, these repeatability data are comparable to those typically observed within commercial standard IC systems and those reported for other IC set-ups aimed towards portability [33,22].

3.4. Assessment of interfering anions

The interference of common anions was studied to ensure no coelution of nitrite and nitrate with other anions was observed when analysing environmental waters. The inorganic anions fluoride, chloride, iodate, iodide, carbonate, sulphate, bromide and phosphate, Cl^-, IO_3^-, I^-, CO_3^{2-}, SO_4^{2-}, Br^- were analysed as they are readily found within natural waters. Of these anions, iodide, iodate and bromide were potentially the most problematic as these anions have absorption spectra extending into the 230 nm region [34]. An anion mixture containing 10 mg L^{-1} of eight typical anions along with nitrite and nitrate was analysed using the simple IC set up coupled with the 235 nm LED detector and custom electronics. The generated chromatogram is shown in Fig. 5. Detection of nitrite and

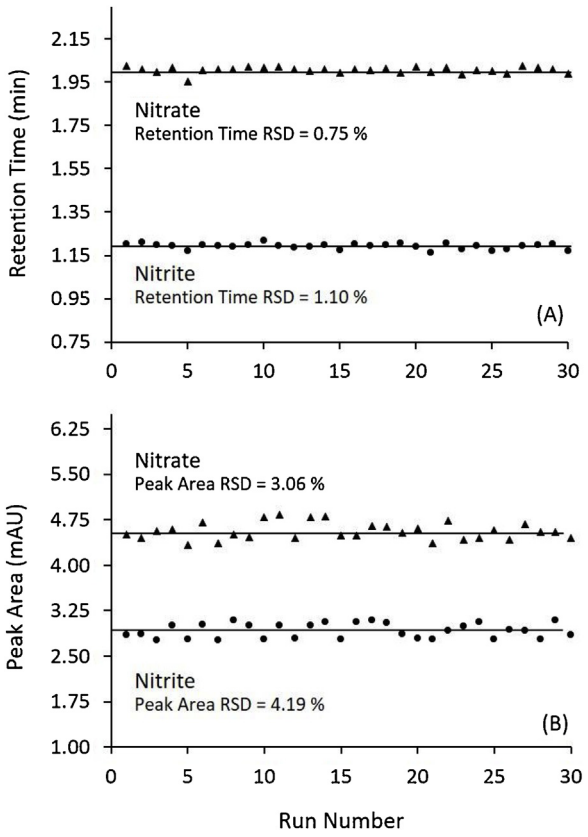

Fig. 4. Repeatability study over 30 sequential runs, analysing 150 μL injection volume of standard containing 0.5 mg L^{-1} NO_2^- and 2.5 mg L^{-1} NO_3^-. Eluent used was 100 mM KOH at a flowrate of 0.8 mL min^{-1} with AG15 guard column for separation. (A) Repeatability of retention times for nitrite and nitrate over runs with associated RSD values. (B) Repeatability of peak area values determined for both analytes over 30 runs and associated RSD values.

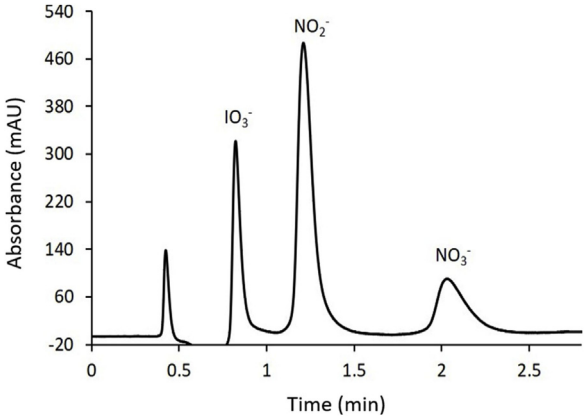

Fig. 5. Chromatogram representing a 150 μL injection volume of 10-anion standard containing 10 mg L^{-1} F^-, Cl^-, NO_2^-, NO_3^-, IO_3^-, I^-, CO_3^{2-}, SO_4^{2-}, Br^- and PO_4^{3-}. The eluent was 100 mM KOH at a flow rate of 0.8 mL min^{-1} using the AG15 guard column as the separator column and 235 nm LED with fabricated optical detection cell.

nitrate was unaffected by the presence of other small inorganic anions. Iodate was the only analyte observed within the 2.5 min elution time, however resolution (R_s) between iodate and nitrite remained sufficient as a R_s value of 2.45 was observed.

3.5. Analytical performance and sample analysis

Under isocratic conditions using 100 mM KOH eluent, an AG15 column and a sample injection volume of 150 μL combined with the 235 nm optical detector with custom electronics both nitrite and nitrate are detected in under 2.5 min. A low backpressure of 11.5 bar was generated by the system, which implies that a lower cost, portable pump could be used. Dynamic linear ranges, using calibration curves based on peak area values and a polynomial fit, were from 0.010 to 15 mg L^{-1} for nitrite and 0.070–75 mg L^{-1} for nitrate, respectively. Calibration plots for each analyte are graphically represented in Fig. C1 – C2 of the ESI. A limit of detection (LOD) of 0.007 mg L^{-1} for NO_2^- and 0.040 mg L^{-1} for NO_3^- was observed, using a signal-to-noise ratio (S/N) of 3 as the threshold [33]. These dynamic linear ranges and LOD values are comparable to those typically reported for commercial benchtop IC systems employing supressed conductivity detection [35,36].

Table 1
Concentrations determined using IC set-up and UV detector versus accredited IC (n = 3).

Sample	Analyte	IC Set-up (mg L^{-1})	Accredited IC (mg L^{-1})	Relative Error (%)
A	Nitrite	1.09 ± 0.014	1.02 ± 0.011	6.86
B	Nitrate	5.14 ± 0.048	5.07 ± 0.054	1.38
Environmental	Nitrite	0.52 ± 0.008	0.50 ± 0.005	4.00
A	Nitrate	4.99 ± 0.051	5.03 ± 0.037	−0.79
Environmental	Nitrite	0.16 ± 0.007	0.15 ± 0.010	6.67
B	Nitrate	61.13 ± 0.403	58.00 ± 0.541	5.40
EPA	Nitrate	53.63 ± 1.08	54.67 ± 0.891	−1.90

A combination of blind standard solutions and environmental samples comprising one river water sample (Environmental A)and one treated effluent water sample from a sugar processing plant (Environmental B) were analysed. The detailed composition of these samples is tabulated in table D1 of the ESI. In addition, an EPA intercalibration solution was also analysed. The intercalibration standard was provided by TelLab and was a standard which is used within the Irish EPA Environmental Intercalibration Programme. This programme assesses analytical performance to ensure validity and comparability of environmental data for laboratories which submit data to the EPA. All samples were first passed through 0.45 μm nylon filters to remove suspended particles. Nitrite and nitrate concentrations determined within each sample using the IC with 235 nm LED detector in comparison to concentrations determined using the accredited IC method are shown in Table 1. The highest relative error observed for nitrite determination was 6.86% and for nitrate was 5.40%. The relative error obtained for the analysis of the EPA intercalibration solution was −1.90%. Although relative errors not exceeding 8.80% were observed when linear calibrations were employed for nitrite and nitrate estimation, by replacing the linear curves with a polynomial fit the total error in terms of the sum of squared residuals (SSR) is reduced by 38.5%. Concentration results obtained using linear calibration curves compared to concentrations obtained by the accredited IC is reported in table E1 of the ESI.

3.6. Integration of detector with low pressure syringe pump

In order to achieve low-cost, portable IC analysis using the developed UV detector and the proposed method, a cost-effective lightweight pumping solution for eluent delivery is required. As a consequence of the low backpressure (11.5 bar) generated by the system, the use of a low-pressure eluent pump is enabled. As a step towards low-cost portable IC analysis using the proposed method, automated syringe pumps were designed, fabricated and coupled with the microinjection valve, AG15 column and the 235 nm LED detection system as shown in Fig. 6. The automated syringe pumps provided eluent delivery and were based on three 1 mL glass syringes housed within 3D printed holders fitted with three brushed DC motors. The design of the eluent syringe pumps is

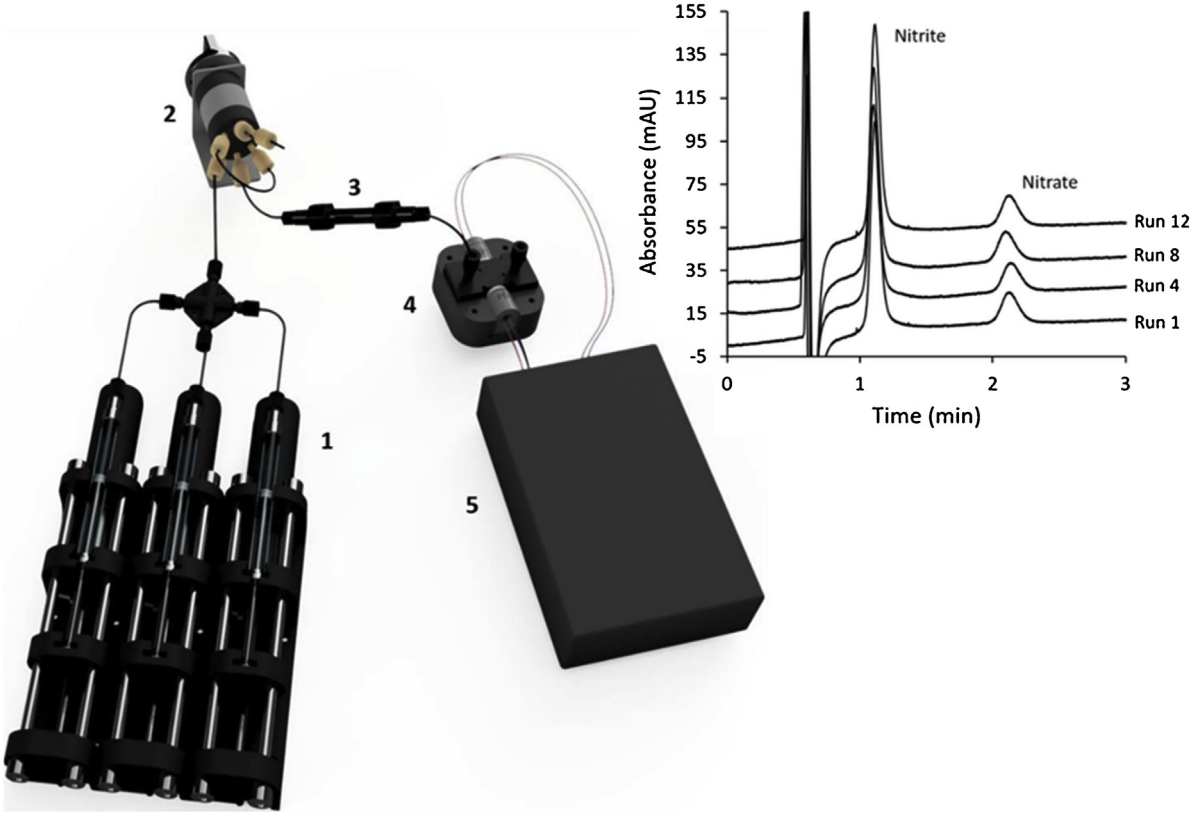

Fig. 6. Illustration of detector, electronics and method coupled with low-pressure syringe pump configuration demonstrating the potential for integration into portable IC format. Legend: (1) Low pressure syringe pumps; (2) manual microinjection valve (3) AG15 guard column; (4) 235 nm LED based UV detector; (5) electronics for LED/PD operation and data acquisition. Selected chromatograms overlaid (offset by 15 mAU) following 12 sequential runs using IC set up with 235 nm LED absorbance detector shown inset. Each chromatogram represents 5 μL injection volume of standard containing 20 mg L^{-1} NO_2^- and NO_3^-. Eluent was 100 mM KOH at a flowrate of 0.7 mL min^{-1} with AG15 guard column.

highlighted in Fig. F1 of the ESI. A voltage of 4.5 V was applied to the motors, attached to the syringe drive plates, which enabled a flowrate of 0.7 mL min^{-1}. The dimensions of the syringe pump configuration were 21 × 13 x 4 cm, with a total weight of <900 g and a cost price of <$235. Selected chromatograms overlaid (offset by 15 mAU) following 12 sequential runs using the automated syringe pump and IC configuration with the 235 nm LED and optical detector are illustrated inset of Fig. 6. RSD values for retention times and peak areas for the 12 runs ranged from 0.80 to 1.15 % and 2.41–3.57 %, respectively. This chromatographic repeatability achieved when using the low-cost, low pressure syringe pump was comparable to that demonstrated when using the 235 nm detector coupled with the commercial HPLC pump (Fig. 4), highlighting the potential of the method and the detector for utilisation within a portable format.

4. Conclusion

A compact, low-cost UV optical detector has been designed and fabricated. Rapid, high sensitivity detection of nitrite and nitrate was achieved by integrating a 235 nm LED with the detector and coupling this detector with a simple, low backpressure IC set up with in-house built electronics for detector control and data acquisition. The detection cell was based on a z-type design and was fabricated through micromilling and solvent vapour bonding of PMMA. The housings for the optical cell and the LED and photodiode were 3D printed, facilitating optical alignment as the holders were fitted into the cell housing. Direct absorbance detection of NO_2^- and NO_3^- was achieved in under 2.5 min under isocratic conditions using 100 mM KOH eluent, an AG15 guard column for separation and the 235 nm LED-based optical detector. The power demand of the LED during analysis was 0.108 W, while a UV deuterium lamp typically employed for direct nitrate and nitrite absorbance detection can have a power demand of 30 W [37]. In addition, as a guard column was used as the separator column, separation was achieved at the low backpressure of 11.5 bar. Both the low power demand demonstrated by the 235 nm LED based detector, along with this low backpressure highlight the potential of the method for implementation within a portable IC analyser.

The need for heat dissipation from thethe 235 nm LED was eliminated when used with this detector as the LED was operated at a low current (<10 mA), enabling stable LED temperatures while analytical performance was maintained. Despite the low-cost nature of the detector, very low stray light and high upper limit of detector linearity was observed. On assessment of chromatographic repeatability, precision comparable to commercial detectors was observed and selective detection for nitrite and nitrate in the presence of other typical small inorganic anions was achieved. The LOD of 0.007 mg L^{-1} for NO_2^- and 0.040 mg L^{-1} for NO_3^- obtained using the low-cost UV detector were comparable to those reported by commercial IC, and dynamic linear ranges suitable for the analysis of almost all natural freshwaters were demonstrated. When compared to an ISO-accredited IC, suitable accuracy was observed as low relative errors (<8.80%) were obtained. The detector and method were also coupled to a low pressure, low cost syringe pump to demonstrate the potential of the system for portable analysis. This simple configuration demonstrated comparable chromatographic repeatability to that achieved when using a commercial HPLC pump.

Future work and development will focus on the design and fabrication of a sample intake system to be coupled with the IC method

and detector. An embedded system will also be developed for integration with the IC method and components to enable system automation and communications towards achieving a low-cost, fully automated in-situ nitrate and nitrite analyser for environmental water monitoring.

Acknowledgements

The authors would like to acknowledge financial support from the Irish Research Council, Grant No. EBPPG/2015/127 and the Australia Awards - Endeavour Research Fellowship, Grant No. 6389_2018. Science Foundation Ireland INSIGHT Centre award SFI/12/RC/2289 is also acknowledged.

Appendix A. Supplementary data

Supplementary material related to this article can be found, in the online version, at doi:https://doi.org/10.1016/j.chroma.2019.05.036.

References

[1] J.A. Camargo, A. Alonso, Ecological and toxicological effects of inorganic nitrogen pollution in aquatic ecosystems: a global assessment, Environ. Int. 32 (2006) 831–849.
[2] Integrated Ocean Observing System, ACT Nutrient Sensor Challenge, 2017 (Accessed 10 October 2018) https://ioos.noaa.gov/news/act-nutrient-sensor-challenge-winners-announced/.
[3] A. Moxey, Agriculture and water quality: monetary costs and benefits across OECD countries, pareto consulting, Edinburgh (2012).
[4] M.J. Moorcroft, J. Davis, R.G. Compton, Detection and determination of nitrate and nitrite: a review, Talanta 54 (2001) 785–803.
[5] Q.H. Wang, L.J. Yu, Y. Liu, L. Lin, R.G. Lu, J.P. Zhu, L. He, L. Lu, Methods for the detection and determination of nitrite and nitrate: a review, Talanta 165 (2017) 709–720.
[6] J.W. O'Dell, Method 353.2: Determination of Nitrate-nitrite Nitrogen by Automated Colorimetry, U.S. Environmental Protection Agency, Cincinnati, 1993.
[7] J. Zhang, P.B. Ortner, C.J. Fischer, Method 353.4: Determination of Nitrate and Nitrite in Estuarine and Coastal Waters by Gas Segmented Continuous Flow Colorimetric Analysis, U.S. Environmental Protection Agency, Washington, 1997.
[8] D.P. Hautman, D.J. Munch, Method 300.1: determination of inorganic anions by ion chromatography, U.S. Environmental protection agency, Cincinnati (1997).
[9] A.D. Beaton, C.L. Cardwell, R.S. Thomas, V.J. Sieben, F.E. Legiret, E.M. Waugh, P.J. Statham, M.C. Mowlem, H. Morgan, Lab-on-Chip measurement of nitrate and nitrite for in situ analysis of natural waters, Environ. Sci. Technol. 46 (2012) 9548–9556.
[10] H. Hwang, Y. Kim, J. Cho, J. Lee, M. Choi, Y. Cho, Lab-on-a-Disc for simultaneous determination of nutrients in water, Anal. Chem. 85 (2013) 2954–2960.
[11] T.M. Schierenbeck, M.C. Smith, Path to impact for autonomous field deployable chemical sensors: a case study of in situ nitrite sensors, Environ. Sci. Technol. 51 (2017) 4755–4771.
[12] Systea S.p.A Analytical Technologies, WIZ Portable In-situ Probe For Water Analysis, 2015 (Accessed 13 October 2018) http://www.systea.it/index.php?option=com_k2&view=item&id=383:wiz-news&lang=en.
[13] s::can Messtechnik GmbH, Spectro::lyser Spectrometer Probe, 2018 (Accessed 13 October 2018) https://www.google.com/search?client=firefox-b-d&q=https%3A%2F%2Fwww.s-+can.at%2Fproducts%2Fspectrometer-probes.
[14] Sea Bird Scientific, SUNA V2 Nitrate Sensor, 2018 (Accessed 13 October 2018) https://www.seabird.com/nutrient-sensors/suna-v2-nitrate-sensor/family?productCategoryId=54627869922.
[15] M. Macka, T. Piasecki, P.K. Dasgupta, Light-emitting diodes for analytical chemistry, Annu. Rev. Anal. Chem. Palo Alto Calif (Palo Alto Calif) 7 (2014) 183–207.
[16] C.M. McGraw, S.E. Stitzel, J. Cleary, C. Slater, D. Diamond, Autonomous microfluidic system for phosphate detection, Talanta 71 (2007) 1180–1185.
[17] M. Sequeira, M. Bowden, E. Minogue, D. Diamond, Towards autonomous environmental monitoring systems, Talanta 56 (2002) 355–363.
[18] S. Schmid, M. Macka, P.C. Hauser, UV-absorbance detector for HPLC based on a light-emitting diode, Analyst 133 (2008) 465–469.
[19] D.A. Bui, B. Bomastyk, P.C. Hauser, Absorbance detector based on a deep UV light emitting diode for narrow-column HPLC, J. Sep. Sci. 36 (2013) 3152–3157.
[20] L. Krčmová, A. Stjernlof, S. Mehlen, P.C. Hauser, S. Abele, B. Paull, M. Macka, Deep-UV-LEDs in photometric detection: a 255 nm LED on-capillary detector in capillary electrophoresis, Analyst 134 (2009) 2394–2396.
[21] Y. Li, P.N. Nesterenko, R. Stanley, B. Paull, M. Macka, High sensitivity deep-UV LED-based z-cell photometric detector for capillary liquid chromatography, Anal. Chim. Acta 1032 (2018) 197–202.
[22] E. Murray, Y. Li, S.A. Currivan, B. Moore, A. Morrin, D. Diamond, M. Macka, B. Paull, Miniaturized capillary ion chromatograph with UV light-emitting diode based indirect absorbance detection for anion analysis in potable and environmental waters, J. Sep. Sci. 16 (2018) 3224–3231.
[23] J. Mack, J.R. Bolton, Photochemistry of nitrite and nitrate in aqueous solution: a review, J. Photochem. Photobiol. A: Chem. 128 (1999) 1–13.
[24] Y. Li, P.N. Nesterenko, B. Paull, R. Stanley, M. Macka, Performance of a new 235 nm UV LED based on-capillary photometric detector, Anal. Chem. 88 (2016) 12116–12121.
[25] M.S. Shur, R. Gaska, Deep-ultraviolet light-emitting diodes, IEEE Trans. Electron Devices 57 (2010) 12–25.
[26] J.F.S. Petruci, M.G. Liebetanz, A.A. Cardoso, P.C. Hauser, Absorbance detector for high performance liquid chromatography based on a deep-UV light-emitting diode at 235 nm, J. Chromatogr. A 1512 (2017) 143–146.
[27] I.R.G. Ogilvie, V.J. Sieben, C.F. Floquet, R. Zmijan, M.C. Mowlem, H. Morgan, Reduction of surface roughness for optical quality microfluidic devices in PMMA and COC, J. Micromech. Microeng. 20 (2010), 065016.
[28] A. Donohoe, G. Lacour, P. McCluskey, D. Diamond, M. McCaul, Development of a cost-effective sensing platform for monitoring phosphate in natural waters, Chemosensors 6 (2018) 57.
[29] M. Macka, P. Andersson, P.R. Haddad, Linearity evaluation in absorbance detection: the use of light-emitting diodes for on-capillary detection in capillary electrophoresis, Electrophoresis 17 (1996) 1898–1905.
[30] C. Johns, M. Macka, P.R. Haddad, M. King, B. Paull, Practical method for evaluation of linearity and effective pathlength of on-capillary photometric detectors in capillary electrophoresis, J. Chromatogr. A 927 (2001) 237–241.
[31] Agilent technologies, incorporated, in: High Sensitivity Detection Cell, 2019 (Accessed 03 January 2019) https://www.agilent.com/en/products/capillary-electrophoresis-ce-ms/ce-ce-ms-supplies/tools-kits-standards/high-sensitivity-detection-cell#productdetails.
[32] S. Sharma, D. Tolley, P.B. Farnsworth, M.L. Lee, LED-based UV absorption detector with low detection limits for capillary liquid chromatography, Anal. Chem. 87 (2015) 1381–1386.
[33] K.R. Elkin, Portable, fully autonomous, ion chromatography system for on-site analyses, J. Chromatogr. A 1352 (2014) 38–45.
[34] Dionex Thermo Scientific, Determination of Nitrite and Nitrate in Drinking Water Using Ion Chromatography With Direct UV Detection, 1991 (Accessed 12 November 2018) https://assets.thermofisher.com/TFS-Assets/CMD/Application-Notes/4189-AU132_Apr91_LPN034527.pdf.
[35] P. Jackson, Determination of Inorganic Anions in Drinking Water by Ion Chromatography, 2015 (Accessed 15 April 2019) https://assets.thermofisher.com/TFS-Assets/CMD/Application-Notes/AN-133-IC-Inorganic-Anions-Drinking-Water-AN71691-EN.pdf.
[36] S.N. Ronkart, Quantification of Trace and Major Anions in Water by Ion Chromatography in a High-Throughput Laboratory, 2012 (Accessed 14 April 2019) https://assets.thermofisher.com/TFS-Assets/CMD/Application-Notes/CAN-114-High-Throughput-IC-Anions-Bromate-LPN3023-EN.pdf.
[37] Thorlabs, Incorporated, Stabilized Deuterium UV Light Source, 2019 (Aaccessed 05 January 2019) https://www.thorlabs.com/newgrouppage9.cfm?objectgroup_id=11783&pn=SLS204.